Distinct and essential morphogenic functions for wall- and lipo-teichoic acids in Bacillus subtilis

The EMBO Journal (2009) 28, 830–842 | © 2009 European Molecular Biology Organization | All Rights Reserved 0261-4189/09
www.embojournal.org

THE
EMBO
JOURNAL

Distinct and essential morphogenic functions for wall- and lipo-teichoic acids in *Bacillus subtilis*

Kathrin Schirner, Jon Marles-Wright, Richard J Lewis* and Jeff Errington*

Centre for Bacterial Cell Biology, Institute for Cell and Molecular Biosciences, The Medical School, Newcastle University, Newcastle upon Tyne, UK

Teichoic acids (TAs) are anionic polymers that constitute a major component of the cell wall in most Gram-positive bacteria. Despite decades of study, their function has remained unclear. TAs are covalently linked either to the cell wall peptidoglycan (wall TA (WTA)) or to the membrane (lipo-TA (LTA)). We have characterized the key enzyme of LTA synthesis in *Bacillus subtilis*, LTA synthase (LtaS). We show that LTA is needed for divalent cation homoeostasis and that its absence has severe effects on cell morphogenesis and cell division. Inactivation of both LTA and WTA is lethal and comparison of the individual mutants suggests that they have differentiated roles in elongation (WTA) and division (LTA). *B. subtilis* has four *ltaS* paralogues and we show how their roles are partially differentiated. Two paralogues have a redundant role in LTA synthesis during sporulation and their absence gives a novel absolute block in sporulation. The crystal structure of the extracytoplasmic part of LtaS, solved at 2.4-Å resolution, reveals a phosphorylated threonine residue, which provides clues about the catalytic mechanism and identifies the active site of the enzyme.

The EMBO Journal (2009) **28,** 830–842. doi:10.1038/emboj.2009.25; Published online 19 February 2009
Subject Categories: cell & tissue architecture; microbiology & pathogens
Keywords: *Bacillus subtilis*; cell wall; lipoteichoic acid; LtaS; protein structure

Introduction

The bacterial cell wall is a crucial structure that represents the interface of the cell with the external medium. It protects the cell from damage, restrains the membrane against the large cellular turgor pressure and confers shape (Koch, 2006). It is essential in almost all organisms for cell division, and in pathogens it is recognized by both the innate and acquired immune systems (Dziarski, 2003). The wall needs to be enlarged to allow growth, while at all times maintaining its integrity (Koch, 1985; Höltje, 1998; Schaffer and Messner, 2005; Stewart, 2005). Peptidoglycan (PG) is a major structure of the walls of virtually all bacteria (Koch, 2006; Vollmer *et al*, 2008) and consists of crosslinked glycan strands forming a complex meshwork surrounding the whole cell. Because of its essential role, PG is the major target for antibiotics such as β-lactams (e.g., penicillins and cephalosporins) and glycopeptides (e.g., vancomycin) (reviewed by Koch, 2003). The walls of Gram-positive bacteria have a second major component, teichoic acid (TA) (Archibald *et al*, 1961). TAs are equally abundant in walls but less well understood (reviewed by Neuhaus and Baddiley, 2003; Bhavsar and Brown, 2006). TAs are anionic polymers and come in two distinct forms depending on whether they are linked to the wall PG (wall TA, WTA) or to the head groups of membrane lipids (lipo-TA, LTA) (Neuhaus and Baddiley, 2003). A wide range of functions that have been proposed for TAs, including: antigenicity and innate immune recognition (Fedtke *et al*, 2004; Seo *et al*, 2008); pathogenicity (Morath *et al*, 2001; Weidenmaier *et al*, 2004; Fittipaldi *et al*, 2008); biofilm formation (Gross *et al*, 2001); efficient release of secreted proteins into the culture medium (Nouaille *et al*, 2004); maintenance of cation homoeostasis (Archibald *et al*, 1961; Heptinstall *et al*, 1970) and antibiotic resistance (Kristian *et al*, 2003; Kovacs *et al*, 2006). Many bacteria have both the WTA and LTA systems, which are synthesized by distinct biochemical routes, even when the actual repeating unit of the polymer is the same (Fischer, 1988). Such is the case for *Bacillus subtilis* strain 168, the subject of this study, in which both WTA and LTA consist of poly(glycerol phosphate) (poly(GroP)) but they are synthesized by separate, genetically distinct pathways (Fischer, 1988; Neuhaus and Baddiley, 2003). Both TAs can carry D-alanyl ester substitutions (reviewed by Neuhaus and Baddiley, 2003).

The WTA system has been relatively well characterized in recent years. The *tagA-F* system encodes enzymes with identified functions for each catalytic step in the biosynthesis of poly(GroP) in the cytoplasm, and then the ABC transporter TagGH apparently exports the polymer for linkage to PG in the cell wall (Mauël *et al*, 1991; Lazarevic and Karamata, 1995; Neuhaus and Baddiley, 2003; Schertzer and Brown, 2003; Bhavsar *et al*, 2004; D'Elia *et al*, 2006a; Formstone *et al*, 2008). WTA was originally thought to be essential because deletions of genes affecting the later steps in the pathway are lethal (Bhavsar *et al*, 2004). However, recent results indicate that the apparent lethality is due to the accumulation of a toxic intermediate. Thus, when *tagO*, encoding the first enzyme in the pathway, is deleted and no intermediates accumulate, the cells are viable though severely compromised (D'Elia *et al*, 2006a, b). Interestingly, the *B. subtilis* mutants appear to be particularly affected in cell elongation (D'Elia *et al*, 2006a). They can still divide but lose the ability to maintain a rod shape and become swollen and almost round. This is consistent with a recent report from this lab that the enzymes of the WTA pathway appear to be

*Corresponding authors. RJ Lewis or J Errington, Centre for Bacterial Cell Biology, Institute for Cell and Molecular Biosciences, The Medical School, Newcastle University, Framlington Place, Newcastle upon Tyne NE2 4HH, UK. Tel.: +44 191 222 8126; Fax: 0191 222 7424;
E-mails: r.lewis@ncl.ac.uk or jeff.errington@ncl.ac.uk

Received: 6 November 2008; accepted: 16 January 2009; published online: 19 February 2009

associated with a cell elongation complex organized by the MreB (actin) system (Formstone *et al*, 2008). The MreB system forms helical filaments that run around the periphery of the cell and appear to insert wall material along helical tracts in such a way as to generate elongation of the rod while maintaining a constant cell diameter (Jones *et al*, 2001; Daniel and Errington, 2003; Stewart, 2005; Carballido-López, 2006; Den Blaauwen *et al*, 2008). *B. subtilis* and many other Gram-positive bacteria have three *mreB* paralogues, the others are known as *mbl* (*mreB* like) and *mreBH* (*mreB* homologue). All three seem to have overlapping, partially redundant functions in cell elongation.

The LTA system and the genes that encode the biochemical pathway are poorly characterized (Perego *et al*, 1995; Gründling and Schneewind, 2007a). Shortly after this study was initiated, Gründling and Schneewind (2007b) reported the discovery of the key enzyme LTA synthase (LtaS), which catalyses the formation of poly(GroP) in *Staphylococcus aureus*. A homologue from *B. subtilis* was shown to possess the same activity and complement the otherwise lethal *ltaS* deletion. We found the *ltaS* gene independently in a screen for suppressors of the Mg^{2+}-dependent growth defect of *mbl* mutants. We show that *ltaS* mutants are affected in divalent cation homoeostasis. The defect leads to shape malformations and to impaired septation and cell division. Therefore, WTA and LTA are largely specialized for different morphogenic systems, elongation and division, respectively. Systematic deletion of the three other *ltaS* paralogues of *B. subtilis* reveals that LTA is essential for spore formation, with a block at the time of polar division and/or progression beyond this step. Quadruple mutants of the *B. subtilis ltaS* paralogues are severely impaired but remain viable. Crucially, complete disruption of the WTA and LTA pathways is lethal, showing that TA synthesis is essential in *B. subtilis*. Finally, we have determined the crystal structure of the extracellular domain of LtaS and identified a catalytic threonine residue, with implications for the biochemical function of the enzyme and potential antibiotic targeting. While this study was in progress, Oku *et al* (2009) showed that LTA and WTA have overlapping and partially redundant roles needed for cell viability and various cell wall properties in *Staphylococcus aureus*.

Results and discussion

Elimination of the LTA synthase YflE suppresses the Mg^{2+} dependency of mbl and mreB mutants

Elsewhere we have shown that *mbl* mutants are not viable at low Mg^{2+} concentrations and that mutations suppressing this phenotype can be readily obtained (Schirner and Errington, 2009). In a collection of transposon-induced suppressed mutants, we found three strains with insertions in the *yflE* gene. Wild-type *yflE* encodes a protein of 649 amino acids with a predicted molecular weight of 74 kDa. DNA sequencing showed that each insertion would disrupt the *yflE* open reading frame, after codons 41, 72 and 387, respectively. While this study was in progress, Gründling and Schneewind (2007b) showed that a closely related gene (79% identical) in S*taphylococcus aureus* encodes LtaS. They also showed that the *yflE* gene of *B. subtilis* could complement the lethal phenotype of *ltaS* in *S. aureus* by restoring LTA synthesis. Therefore, we subsequently refer to the *B. subtilis yflE* gene as *ltaS*.

It was not clear why disruption of *ltaS* suppressed the Mg^{2+} sensitivity of the *mbl* mutant. However, after more than two decades of speculation about the possible function of LTA, identification of a gene specifically required for LTA synthesis provided us with an important opportunity to investigate the physiological role of these polymers in *B. subtilis*. We first constructed a strain in which the *ltaS* gene was completely deleted and then confirmed that the *ltaS mbl* double deletion strain grows on plates at normal Mg^{2+} levels, unlike the *mbl* single mutant (Figure 1A). In liquid PAB medium with no added Mg^{2+} (Figure 1B; or in LB, not shown), the double mutant (circles) grew much better than the *mbl* mutant (squares), although growth was slower than for the wild-type culture (diamonds). Deletion of *ltaS* also counteracted the typical swelling and extreme twisting of *mbl* mutant cells; instead, the double mutant appeared similar to the *ltaS* single mutant (Figure 1C) (see below).

mreB mutants and, to a much lesser degree *mreBH*, have also been shown to be sensitive to Mg^{2+} levels (Formstone and Errington, 2005; Carballido-López, 2006). Combination of *ltaS* with an *mreB* disruption also led to the restoration of growth and morphology on nutrient agar (NA) plates, on which *mreB* mutants do not grow (Formstone and Errington, 2005), and in liquid PAB medium (data not shown). An *ltaS mreBH* double mutant was not detectably different from the

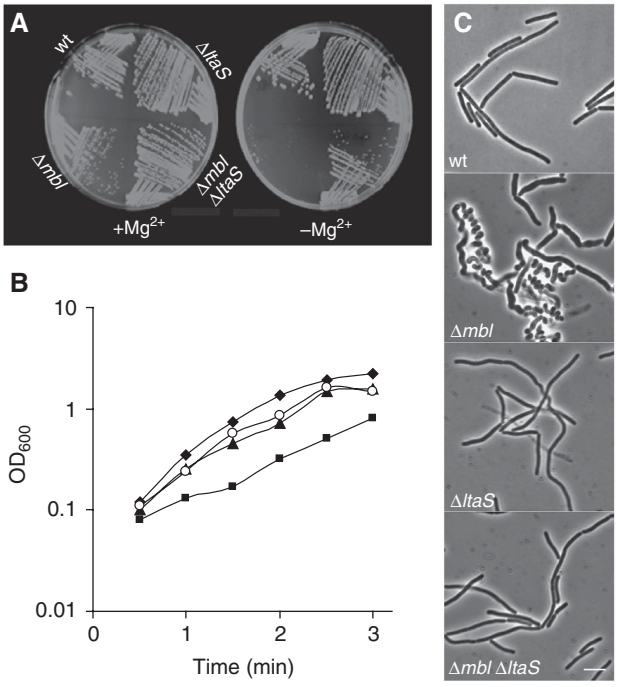

Figure 1 Deletion of *ltaS* suppresses the Mg^{2+} dependency of *mbl* mutants. (**A**) Growth of wild type (168), *mbl* mutant (2505), *ltaS* mutant (4283) and suppressed *mbl* mutant (Δ*mbl* Δ*ltaS*, 4298) on NA plates with (left) or without (right) addition of 20 mM Mg^{2+}. (**B**) Growth curves of wild type (168, ◆), *mbl* mutant (2505, ■), *ltaS* mutant (4283, ▲) and suppressed *mbl* mutant (Δ*mbl* Δ*ltaS*, 4298, ○) in PAB medium at 37°C. (**C**) Phase-contrast microscopy of wild type (168), *mbl* mutant (2505), *ltaS* mutant (4283) and *mbl ltaS* double mutant (4298) grown in PAB medium at 37°C. Scale bar 5 μm.

isogenic *ltaS* single mutant in growth or morphology (though the phenotype of *mreBH* mutants is mild).

Altered susceptibility to divalent cation levels in ltaS mutants

Although the *ltaS* single mutant also grew slightly more slowly than the wild type in PAB medium (doubling time 31 versus 26 min; Figure 1B), we were surprised to find that growth was almost abolished in two of our other standard growth media, CH and S-medium. By adding components of these media to PAB, it emerged that the mutant strain was unusually sensitive to Mn^{2+}. In the examples shown in Figure 2A, addition of 0.05 mM $MnSO_4$ to NA abolished growth of the mutant, whereas growth of the wild type was unaffected. Addition of 0.5 mM Mg^{2+} had no effect on growth of the mutant, showing that the effect was not a general sensitivity to divalent cations. In fact, we noticed that the mutant had a reduced requirement for Mg^{2+}, at least on minimal agar (Figure 2B). Thus, under these conditions the mutant strain grew better than the wild type at both 10 and 100 μM Mg^{2+}. The lowered requirement for Mg^{2+} may be the reason why a deletion of *ltaS* suppresses the Mg^{2+}-dependent phenotype of both *mbl* and *mreB* mutants (Formstone and Errington, 2005). These results provide strong support for a model in which LTA is important in scavenging and sequestration of Mg^{2+} ions (Neuhaus and Baddiley, 2003). Loss of the LTA-dependent buffering zone in the cell wall allows divalent cations more immediate access to the cell surface. This in turn leads to a lower requirement for Mg^{2+}, which is a cofactor in many enzymes, and increased susceptibility to toxic Mn^{2+} ions, which can replace Mg^{2+} because of their similar physicochemical properties but which often cannot substitute for Mg^{2+} in enzyme function (Cowan, 1995). These results suggest that LTA helps to provide a physicochemical environment that favours the retention of Mg^{2+} over Mn^{2+} in the cell wall.

In the process of constructing the deletion strain, we noticed that the *ltaS* mutant was also hypersensitive to various antibiotics (Supplementary Table 2) and lysozyme (data not shown). The effect was not specific to a certain class of antibiotic, suggesting that LTA also provides a protective layer that restricts the access of many bioactive agents to sensitive sites in the cell envelope.

Defective cell division in ltaS mutants

Microscopic examination of *ltaS* mutant cells grown under various conditions revealed a characteristic phenotype. This did not appear to be affected by the presence or absence of added Mg^{2+} or Mn^{2+}, so all further experiments described were based on unsupplemented PAB medium unless stated otherwise. The main morphological effects (Figure 1C) were increased cell or cell chain length (*B. subtilis* has a tendency to form chains of cells, due to a delay between cell division and separation of sister cells; Paulton, 1971), reduced cell diameter (~90% of that of wild-type cells; Table I) and a significant frequency of cell bending and lysis (Figure 1C). The reduced cell width has been seen previously for mutants affected in cell envelope systems (e.g., Carballido-López *et al*, 2006), but its significance is not yet understood. In membrane-stained preparations, it was evident that the elongated appearance was at least partly due to an effect on cell division, with long aseptate regions occurring at irregular

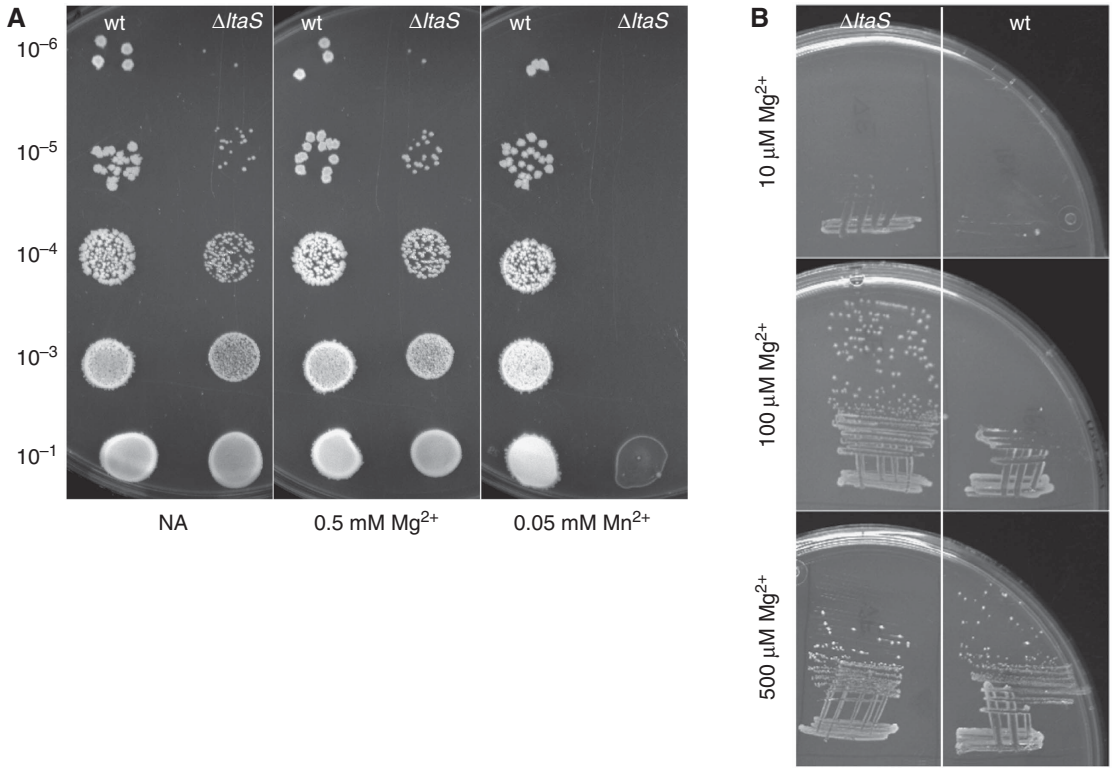

Figure 2 Effect of metal ion concentration on the viability of wild type and *ltaS* mutants. (**A**) Growth of wild type (168) and *ltaS* mutant (strain 4286) on NA plates (left panel) containing 0.05 mM Mg^{2+} (middle panel) or 0.5 mM Mn^{2+} (right panel). The strains were grown to mid-exponential phase and spotted onto the plates in the dilutions as indicated. (**B**) Growth of *ltaS* mutant (strain 4283, left) and wild type (strain 168, right) on minimal medium plates containing 10, 100 and 500 μM Mg^{2+} as indicated.

Table I Effects of mutations in *lta* genes on cell diameter

Strain	Genotype	Average cell diameter (μm) ± s.d.	Range (μm)
168	wt	0.85 ± 0.07	0.67–1.04
4283	Δ*ltaS*	0.75 ± 0.08	0.57–0.98
4287	Δ*yfnI*	0.84 ± 0.06	0.66–1.02
4292	Δ*yqgS*	0.84 ± 0.05	0.67–0.99
4295	Δ*yvgJ*	0.87 ± 0.04	0.73–0.98
4610	Δ*ltaS* Δ*yfnI*	0.78 ± 0.09	0.54–1.10
4611	Δ*ltaS* Δ*yqgS*	0.76 ± 0.07	0.54–0.96
4612	Δ*ltaS* Δ*yvgJ*	0.74 ± 0.05	0.60–0.93
4613	Δ*yfnI* Δ*yqgS* Δ*yvgJ*	0.81 ± 0.06	0.68–1.00
4620	Δ*ltaS* Δ*yfnI* Δ*yqgS* Δ*yvgJ*	0.85 ± 0.09	0.66–1.16
4298	Δ*ltaS* Δ*mbl*	0.80 ± 0.06	0.67–0.97

Cells were grown in PAB medium to exponential phase, stained with Nile Red, and cell width was measured using ImageJ.

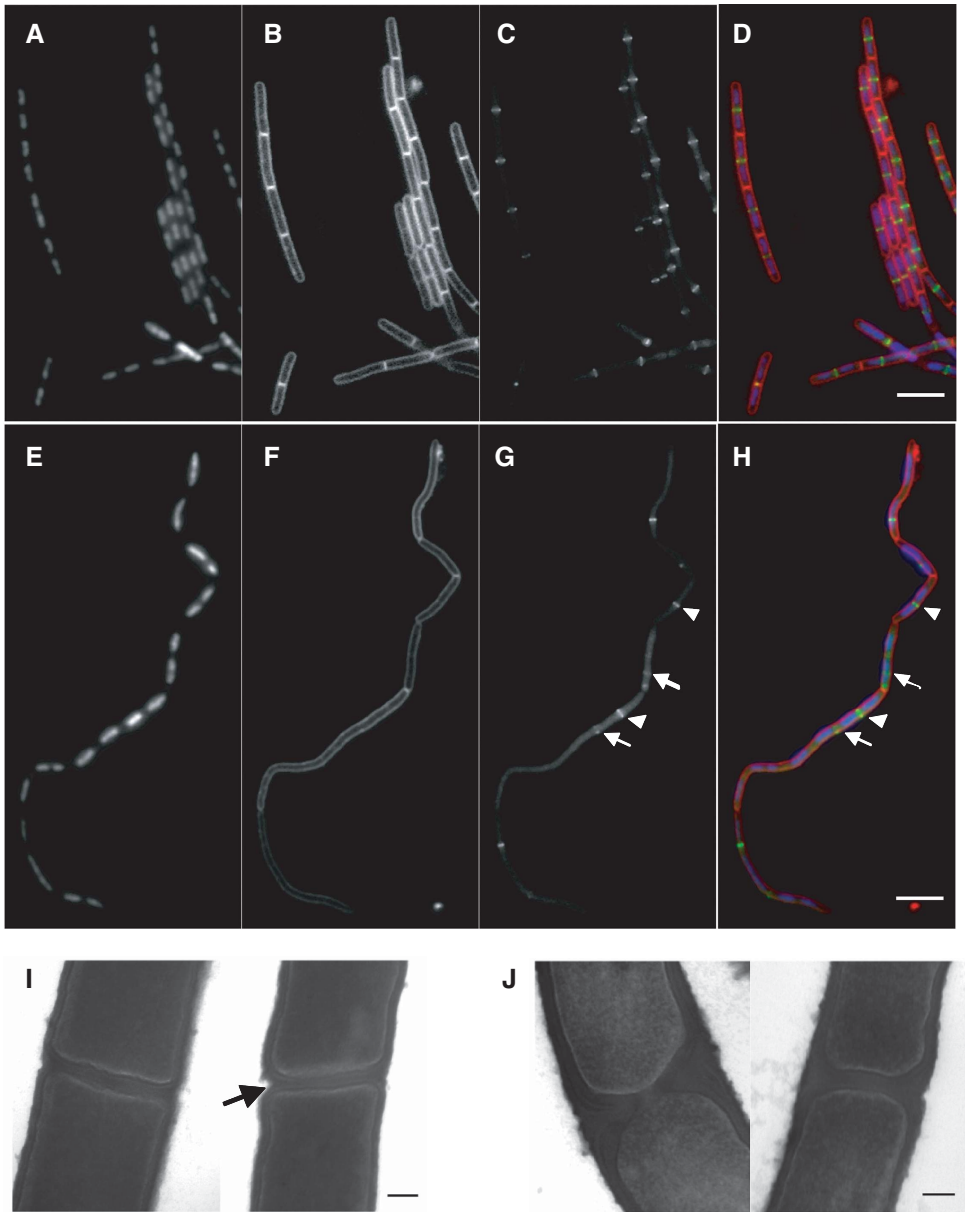

Figure 3 Effects of *ltaS* mutation on FtsZ ring formation, cell division and cell separation. The strains were grown to mid-exponential phase in PAB medium at 30°C (**A**–**H**) or 37°C (**I**, **J**). (A–H) Samples of wild type (strain 2020; A–D) and *ltaS* mutant (4605; E–H) carrying *gfp-ftsZ* under a xylose-inducible promoter were stained with DAPI (for DNA) and FM5-95 (for the membrane), and additionally imaged for FtsZ–GFP localization. (D, H) Overlays of the membrane (red), DNA (blue) and GFP (green) signals. Scale bar 5 μm. (**I**, **J**) Transmission electron microscopic images of transverse sections of two representative septa each of wild type (168; I) and *ltaS* mutant (strain 4284; J). Scale bar 100 nm.

intervals in the chains (compare images of wild type and mutant in Figure 3B and F). Interestingly, the effect on division was exerted at an early step in the process. Assembly of FtsZ protein into a ring at sites of impending division is the earliest marker for cell division (reviewed by Dajkovic and Lutkenhaus, 2006). In wild-type cells, bands (which correspond to rings seen edge-on) of FtsZ–GFP are formed at regular positions between segregating nucleoids (Figure 3C). In contrast, FtsZ–GFP localization was deranged in the *ltaS* mutant (Figure 3G). When clear bands of FtsZ–GFP were observed, they were usually correctly positioned between well-separated nucleoids (arrowheads). However, FtsZ–GFP bands were either missing or only present as faint bands (arrows) at many potential division sites, and there appeared to be a higher than normal background of non-localized fluorescence. DAPI staining showed that chromosomes were replicating and segregating more or less normally in the mutant, suggesting that the division defect was not secondary to a chromosome segregation defect (Figure 3A and E).

Transmission electron microscopy (TEM) revealed that the morphology of the division septa formed in *ltaS* mutants was abnormal. In the typical examples shown in Figure 3I and J, the wild-type septum was of fairly uniform thickness and the membranes at the nascent sister cell poles were rather flattened, curved only near their outer edges at the junction with the lateral wall (Figure 3I). In contrast, the mutant septa were abnormally thick, especially towards their outer edges, with unusual triangular wedges of wall material (Figure 3J). Furthermore, it appeared that the autolytic activity that leads eventually to cell separation (Blackman *et al*, 1998) and which usually begins at the outer edges of the septa (arrowed for the wild-type cell in Figure 3I), was delayed in the *ltaS* mutant. Autolytic enzyme activity has previously been suggested to be regulated by anionic polymers and the ionic environment of the cell wall (Cheung and Freese, 1985; Wecke *et al*, 1997; Smith *et al*, 2000). *ltaS* mutants therefore have important defects in both formation of the cell division septum and subsequent cell separation. We suggest that these defects occur, at least in part, because the impaired cation homoeostasis interferes with proper regulation of the activities of the enzymes that carry out the synthesis and turnover of the wall at division sites.

Partial functional redundancy of LtaSs in B. subtilis

A most likely explanation for the viability of the single *ltaS* mutant was that *B. subtilis* has three paralogues of *ltaS*, namely *yfnI*, *yqgS* and *yvgJ*. These genes encode products predicted to be about 53, 44 and 41% identical to LtaS, respectively (based on BLAST searches run on the SubtiList web server (Moszer *et al*, 2002). Only expression of *ltaS*, however, restored LTA synthesis in an *S. aureus ltaS* deletion strain (Gründling and Schneewind, 2007b). We constructed null mutants for each of the three paralogues and examined their microscopic and growth phenotypes. None of the single mutants had a discernible effect on growth rate or cell morphology (Supplementary Figure 1B, D–H). Combinations of mutations were then made. All double mutants combining with *ltaS* were comparable in growth and morphology to the single *ltaS* mutant, and a triple Δ*yfnI* Δ*yqgS* Δ*yvgJ* mutant did not differ noticeably from the wild type (data not shown).

Surprisingly, we were readily able to construct a strain in which all four *ltaS* paralogues were disrupted, indicating that, in contrast to *S. aureus*, LTA is not essential in *B. subtilis*. However, the phenotype of the quadruple mutant Δ*ltaS* Δ*yfnI* Δ*yqgS* Δ*yvgJ* was more severe than that of the *ltaS* single mutant: the mutant strain grew very slowly with a doubling time of about 48 min in PAB medium at 37°C, whereas the doubling time of the *ltaS* single mutant was around 31 min, and the wild type doubled every 26 min under the same conditions (Supplementary Figure 1C). The quadruple mutant also had a severe cell division and cell separation defect, resulting in the formation of filamentous clumps of cells; the cell filaments were tightly twisted around their long axis and lysis of cell compartments was common (Supplementary Figure 1I). Taken together, these observations support the idea of a partial functional redundancy of the four LtaS-like proteins.

Interestingly, the coiling and clumping of the strain lacking LTA were reminiscent of the *mbl* mutant phenotype. We suggest, that in both strains an imbalance of processes involved in cell wall synthesis or modifications of the electrostatic properties of the wall lead to twisting and macrofibre formation (Mendelson *et al*, 1985).

Analysis of the expression of these genes through fusions to *lacZ* revealed that *ltaS* was expressed much more strongly than the other genes under normal growth conditions (Supplementary Figure 1A). In previous proteomic studies (Hirose *et al*, 2000), LtaS and YfnI, but neither YqgS nor YvgJ, were detected in growing cells. Transcription of *yfnI* is dependent on the extracytoplasmic sigma factor σ^M (Jervis *et al*, 2007), which is involved in salt stress resistance. However, we did not detect any effect of salt stress on the *yfnI* single mutant, nor on the *ltaS yfnI* double mutant (not shown).

These results indicate that LtaS is the major LTA synthase, whereas the other three paralogues have a minor function and might be required for adaptation to specific environmental or developmental conditions.

Specific and essential requirement for LtaS during stages II–III of sporulation

Although the four single mutants (Δ*ltaS*, Δ*yfnI*, Δ*yqgS* and Δ*yvgJ*) were sporulation proficient, we were surprised to find that the *ltaS yqgS* double mutant did not form spores, as

Table II Effects of *lta* mutations on sporulation frequency

Strain	Genotype	% sporulation (no. of cells counted)
168	wt	57 (2415)
4283	Δ*ltaS*	47 (1425)
4287	Δ*yfnI*	57 (2719)
4292	Δ*yqgS*	56 (3796)
4295	Δ*yvgJ*	61 (1972)
4610	Δ*ltaS* Δ*yfnI*	41 (2719)
4611	Δ*ltaS* Δ*yqgS*	<0.07 (1536)
4612	Δ*ltaS* Δ*yvgJ*	2.1 (3676)
4613	Δ*yfnI* Δ*yqgS* Δ*yvgJ*	45 (4043)
4627	Δ*ltaS* Δ*yqgS* P_{xyl} *gfp-ltaS*	43 (2083)
4628	Δ*ltaS* Δ*yqgS* P_{xyl} *gfp-ltaS T297A*	<0.03 (3578)

Cells were grown in Schaeffer's medium for 24 h, and then sporulation efficiency was determined by microscopic counting.

judged by phase-contrast microscopy (Table II). In contrast, the other double mutants in combination with *ltaS* did sporulate, although the *ltaS yvgJ* mutant had a reduced efficiency (Table II). The triple mutant Δ*yfnI* Δ*yqgS* Δ*yvgJ* sporulated almost similar to the wild type. Remarkably, when a more sensitive method was used to measure the spore frequency (numbers of heat- or chloroform-resistant spores formed in liquid culture), spores could not be detected for the *ltaS yqgS* double mutant ($<10^{-7}$ spores per viable cell; under the same conditions we observed over 0.6 spores per viable cell for the *ltaS* single mutant). Such a severe sporulation block is normally associated only with mutations that eliminate key regulatory proteins or proteins involved in critical morphological or structural changes that occur during spore development (Piggot and Coote, 1976; Errington, 1993). These results suggested that LTA is essential for sporulation and that expression of the minor LtaS, *yqgS*, provides sufficient activity to compensate for loss of the major LtaS, *ltaS*. Disruption of both genes results in the severe sporulation defect.

Preliminary microscopic examination suggested that sporulation was arrested at stage II, when a division septum is formed near one pole of the cell. Activation of a key transcription factor, the sigma factor, σ^F, is dependent on the formation of the septum (reviewed by Errington, 1993; Hilbert and Piggot, 2004), so we tested whether the synthesis and activation of σ^F were affected by *ltaS yqgS* disruption. *lacZ* and *mCherry* fusions to the *spoIIA* promoter, which drives expression of the operon that encodes σ^F, showed that *spoIIA* was efficiently activated to similar levels as in the *ltaS* single mutant (Figure 4A and data not shown). In contrast, expression of a *lacZ* reporter gene fusion to a promoter that is dependent on active σ^F (that of *spoIIQ*) was completely blocked in the double mutant (Figure 4B). Similarly, the natural reporter enzyme alkaline phosphatase (AP), which depends on σ^F indirectly through activation of

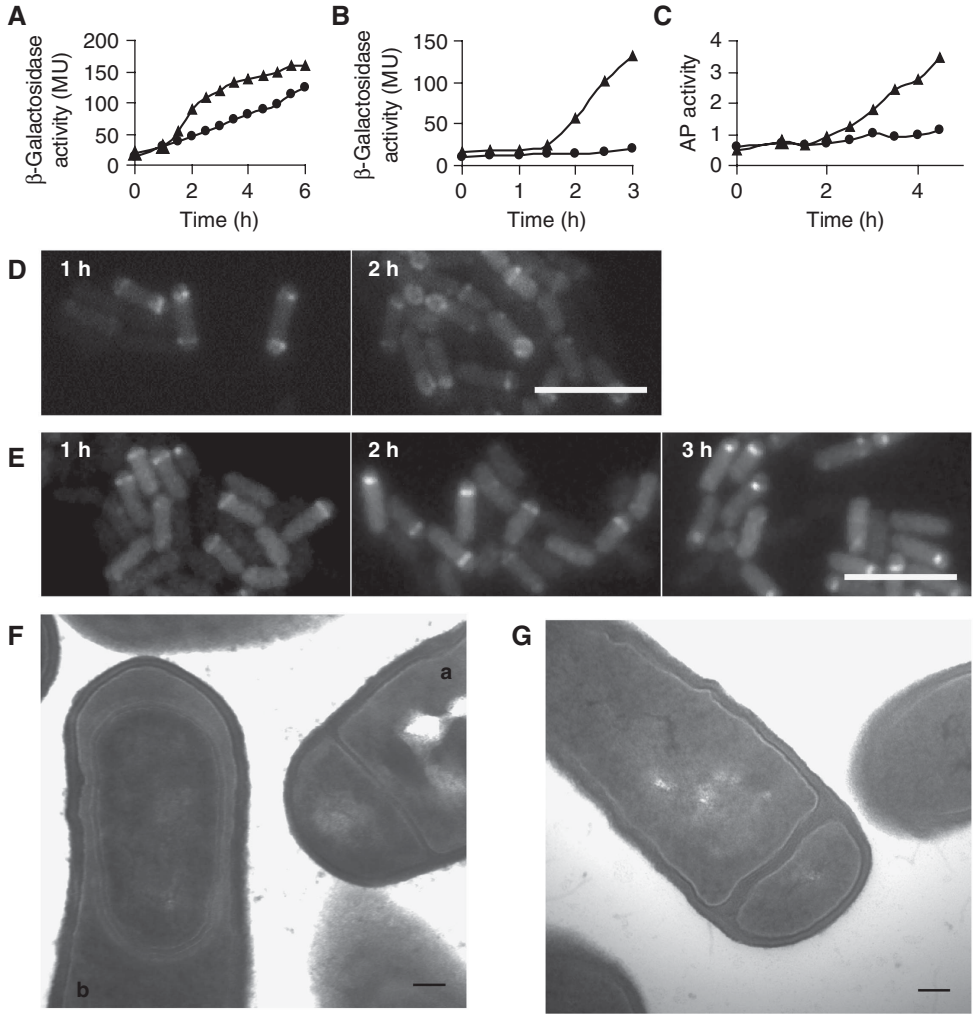

Figure 4 Effects of *ltaS* and *yqgS* deletion on sporulation. (**A**) Expression pattern of the *spoIIA* promoter measured by assaying β-galactosidase activity of strains 4614 (*ltaS* mutant, ▲) and 4615 (*ltaS yqgS* double mutant, ●) grown in Schaeffer's medium at 37°C. (**B**) Measurements of β-galactosidase activity of strains *ltaS* mutants (4616, ▲) and *ltaS yqgS* double mutants (4617, ●) carrying the *lacZ* gene under control of the σ^F-inducible *spoIIQ* promoter. (**C**) Assay for sporulation-specific alkaline phosphatase activity in *ltaS* mutant (4283, ▲) and *ltaS yqgS* double mutant (4611, ●). All strains were grown in Schaeffer's medium at 37°C, time point 0 was set at the entry into stationary phase (A–C). (**D**, **E**) Localization of SpoIIE–GFP in an *ltaS* mutant background (strain 4618 (D)) and an *ltaS yqgS* double-mutant background (strain 4619 (E)). Time was measured from the point at which fluorescence of *mCherry* (under control of the *spoIIA* promoter) first became visible and images were taken at the time points indicated. Scale bar 5 μm. (**F**, **G**) Transmission electron microscopic images of sporulating cultures of *ltaS* mutant (4284 (F); asymmetric septum is marked 'a', engulfed forespore is marked 'b') and *ltaS yqgS* double mutant (4611 (G)). The strains were grown for 9 h in Schaeffer's medium at 37 before fixation. Scale bar 100 nm.

σ^E (Glenn and Mandelstam, 1971; Piggot and Coote, 1976; Stragier *et al*, 1984; Illing and Errington, 1991) was also blocked by the *ltaS yqgS* double deletion (Figure 4C). This effect was not due to a failure in translocation of the prespore chromosome (Wu and Errington, 1994), based on (i) DAPI staining (data not shown) and (ii) the fact that the *spoIIQ–lacZ* fusion was located at *amyE*, which is captured in the prespore compartment even when chromosome translocation fails (Wu and Errington, 1994).

A key player in the machinery regulating σ^F activation is SpoIIE. This protein has a dual role in sporulation, being required for proper formation of the polar septum and for the correct spatial and temporal activation of σ^F (reviewed by Errington, 2003; Hilbert and Piggot, 2004). Expression of *spoIIE* is turned on during the early stages of sporulation (stage 0) and its product is targeted to the polar division sites (Arigoni *et al*, 1995; Barak *et al*, 1996; Wu and Errington, 1998). We therefore examined the effects of the *ltaS yqgS* deletion on synthesis and targeting of SpoIIE through a *spoIIE-gfp* fusion. As expected, SpoIIE–GFP was expressed in both single and double-mutant cells (Figure 4D and E). The SpoIIE–GFP fusion also appeared to target to the polar septa that were formed in the double-mutant cells as well as in the single mutant. However, in the *ltaS yqgS* double mutant, SpoIIE–GFP remained static at the asymmetric septa (Figure 4E), whereas in the *ltaS* single mutant it progressed rapidly to the next step of spore development, engulfment of the prespore (ovoid GFP signals in the 2 h image in Figure 4D). Taken together, these results suggest that the block in sporulation occurs in the signalling pathway for σ^F activation, but downstream of SpoIIE synthesis and recruitment to the polar septum.

As σ^F activation is thought to be coupled to polar septation and vegetative division septa were abnormal in the *ltaS* single mutant, we questioned whether the double mutant might be affected in the ultrastructure of the polar septum. TEM images of culture samples taken 4 h after initiation of sporulation showed that the *ltaS* single mutant formed apparently normal, thin asymmetric septa, similar to those of wild-type cells (cell marked 'a' in Figure 4F) (Hilbert and Piggot, 2004). We also noticed that many cells went on to engulf the prespore in a typical manner (Figure 4F, cell 'b'). In contrast, the septa of the *ltaS yqgS* double mutant were highly abnormal. In the typical example shown (Figure 4G), the septum was much thicker than normal, almost the same as in vegetative cells (compare to Figure 3I), and is reminiscent of the abnormal septa of *spoIIE* mutant cells (Illing and Errington, 1991; Khvorova *et al*, 1998; Carniol *et al*, 2005) or a *divIB* mutant (Thompson *et al*, 2006). The presence of highly abnormal polar septa in the double mutant, but not in the *ltaS* single mutant, provided a likely explanation for the failure in σ^F activation and suggests that LTA is a key component in the polar sporulation septum upon which the pivotal cell-specific σ^F activation mechanism is strictly dependant. Therefore, these results point to an important role for LTA synthesis in cell division of both vegetative and sporulating cells. The results also suggest that the *ltaS* paralogues contribute to LTA function differently, with *yfnI* supporting *ltaS* function during vegetative growth and *yqgS* and *yvgJ* acting in stationary phase. The molecular basis for the block in σ^F activation remains to be resolved.

LtaS and YqgS localize predominantly at division sites in both vegetative and sporulating cells

The results described above suggest an important role for LTA in cell division, of both vegetative and sporulating cells. If true, the synthases ought to be localized at division sites, at least in part. A range of predictive bioinformatic tools, such as TMpred (Hofmann and Stoffel, 1993) predict that LtaS and its paralogues have five transmembrane domains near their N termini, followed by a large C-terminal extracellular domain, which contains the catalytic centre responsible for poly(GroP) synthesis (see below). GFP fusions to LtaS and YqgS were at least partially functional as judged by restoration of wild-type growth rate and cell shape (GFP–LtaS) and sporulation proficiency (both fusions expressed in the appropriate deletion backgrounds). Although the fusions gave relatively weak fluorescence signals, they were clearly associated with the cell periphery. Importantly, both proteins appeared to be enriched at division sites, in both vegetative and sporulating cells (Figure 5A and B). As the double-mutant cells produced septa that resembled those of *spoIIE* mutants (see above) it was possible that the SpoIIE phenotype was due to delocalized YqgS. However, GFP–YqgS still localized to polar septa in a *spoIIE* deletion background (Figure 5C). Indeed, fluorescence was often clearly visible at polar septa near both cell poles; a phenotype characteristic of *spoIIE* mutants (Piggot and Coote, 1976; Illing and Errington, 1991). These results support the idea that LTA synthesis is particularly important for cell division.

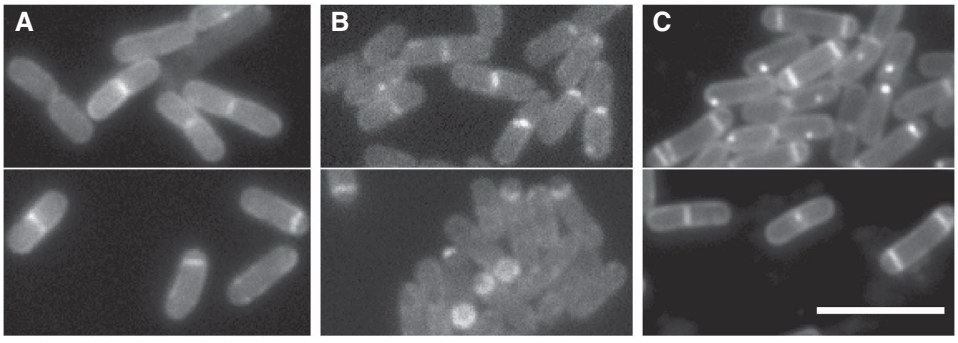

Figure 5 GFP–LtaS and GFP–YqgS localization. Fluorescence microscopy of strains 4607 and 4609 carrying inducible alleles of *gfp-ltaS* (**A**) and *gfp-yqgS* (**B**) at the *amyE* locus. Localization of GFP–YqgS in an *spoIIE* mutant background (strain 4626 (**C**)). Of each strain two fields are shown, all strains were grown in S-medium containing 0.5% xylose at 30°C. Scale bar 5 μm.

Evidence that LTA and WTA have specialized functions in cell morphogenesis

The phenotype of cells devoid of LTA differs clearly from that previously reported for deficiency in WTA. The latter mutants, for example in *tagO* or *tagF*, typically become bloated and spherical (Wagner and Stewart, 1991; D'Elia *et al*, 2006a), but are still capable of division, as can many other mutants with a specific defect in cell elongation (Henriques *et al*, 1998; Wei *et al*, 2003; Leaver and Errington, 2005). Consistent with this role, the localization of several Tag proteins, particularly TagG and TagH, suggests that they might be associated with the cell elongation machinery (Formstone *et al*, 2008). In contrast, the above results showed that LTA-deficient mutants have a distinct and almost complementary phenotype, in efficiently elongating along a longitudinal growth axis (albeit with a considerable level of twisting) but clearly impaired in cell separation and cell division.

We were now in a position to test the effects of loss of both TA systems in *B. subtilis*. First, we introduced a deletion in the major LtaS gene, *ltaS*, into a *tagO* deletion strain. The resultant strain was viable and phenotypically resembled the *tagO* single mutant in being rounded and growing in clumps (Figure 6B; compare with Figure 6A) (D'Elia *et al*, 2006a). Attempts to combine all four *ltaS* mutations and *tagO* failed, suggesting that this combination might be lethal. We therefore constructed a strain in which *ltaS* was controlled by a xylose-inducible promoter. We then deleted the other three *ltaS* paralogues, and were able to introduce the *tagO* deletion in the presence of xylose. Results shown in Figure 6E confirmed that inactivation of both the LTA and WTA systems was indeed lethal. The P_{xyl}-*ltaS* strain (4622) grew well in the presence or absence of xylose. Combined with the triple deletion of the other *ltaS* paralogues (strain 4623), growth was still reasonable, though slightly reduced in the absence of xylose. The *tagO* P_{xyl}-*ltaS* mutant (strain 4624) grew poorly on both the xylose and non-xylose plates, but when the triple deletion was also present (strain 4625), growth in the absence of xylose was abolished. The two *tagO* P_{xyl}-*ltaS*-containing mutants (with and without the triple deletion) were then cultured in liquid PAB medium ($+Mg^{2+}$) with and without xylose (Figure 6F). The growth rate of the *tagO* P_{xyl}-*ltaS* mutant was reduced but still detectable in the absence of xylose (open triangles), but the pentuple mutant failed to grow at all in the absence of inducer (open circles). Figure 6C shows that the morphological appearance of the pentuple mutant in the presence of xylose was similar to that of the other *tagO* mutants, except that the cells were somewhat larger and even more clumped. Cells cultured for several hours in the absence of xylose showed little differences in morphology, suggesting that growth was arrested without any further change in morphology (Figure 6D). The lethality arising from loss of both TA systems shows that synthesis of anionic polymers is essential for *B. subtilis*. There are two ways in which this lethality might arise, which we cannot yet distinguish. The first possibility is that complete loss of anionic polymer synthesis affects divalent cation homoeo-

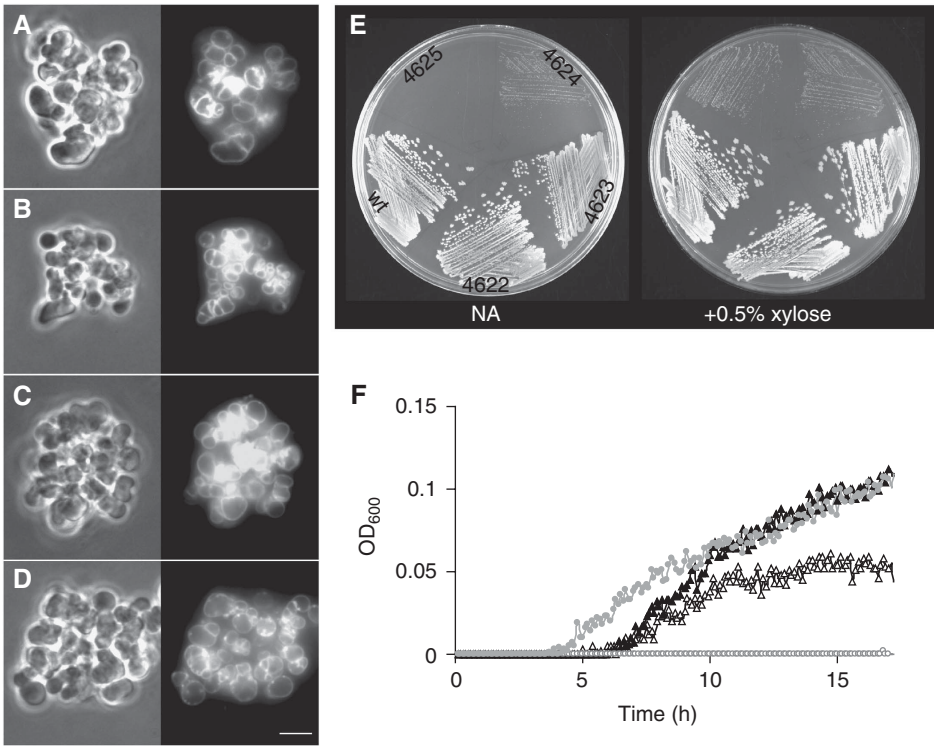

Figure 6 Morphology and viability of LTA and WTA mutants. (**A**–**D**) Morphology of a *tagO* mutant (strain 4282 (A)) and an *ltaS tagO* double mutant (strain 4621 (B)). Strain 4625 growing in the presence of 0.5% xylose (C) and after depleting for xylose (D). Left panels show phase-contrast microscopic images, right panels show staining of the membrane with FM5-95. The strains were grown in PAB medium with the addition of 10 mM Mg^{2+} at 37°C, scale bar 5 μm. (**E**) Strains 4622 (P_{xyl}-*ltaS*), 4623 (Δ*yfnI* Δ*yqgS* Δ*yvgJ* P_{xyl}-*ltaS*), 4624 (Δ*tagO* P_{xyl}-*ltaS*), 4625 (Δ*tagO* Δ*yfnI* Δ*yqgS* Δ*yvgJ* P_{xyl}-*ltaS*) and wild type (168) were cultured on NA with (right) or without 0.5% xylose (left) overnight at 37°C. (**F**) Growth curve of strains 4624 (Δ*tagO* P_{xyl}-*ltaS*, ▲) and 4625 (Δ*tagO* Δ*yfnI* Δ*yqgS* Δ*yvgJ* P_{xyl}-*ltaS*,) in PAB medium containing 10 mM Mg^{2+} with (closed symbols) or without (open symbols) addition of 0.5% xylose. The cultures were grown in a microtitre plate while shaking at 37°C.

stasis so badly that multiple enzyme systems are inhibited resulting in growth arrest. The second is that impairment of both the elongation- and division-associated wall synthetic systems eliminates all routes to growth.

Crystal structure of LtaS$_{215–649}$

LtaS has an important function in the morphology and physiology of *B. subtilis*. To gain insights into the enzymatic function performed by LtaS, we solved the structure of the extracellular domain (residues 215–649, LtaS$_{215–649}$) by X-ray crystallography using a selenomethionine-substituted sample and anomalous scattering procedures. The experimental SAD electron density maps were of such quality that the entire structure of the domain, bar the last 14 amino acids, could be built and refined to convergence. The two independent molecules in the asymmetric unit are indistinguishable and can be considered equal. Details of the data collection, structure solution and refinement are in Table III.

Globally, LtaS$_{215–649}$ belongs to the AP superfamily (Millán, 2006), despite sharing only ~15% sequence identity to its closest structural neighbours in the PDB (Figure 7A). The core of LtaS$_{215–649}$ is an α/β-fold, common to all its structural homologues. The nearest homologue is an unpublished output from a structural genomics effort (PDBid 3ed4), which is annotated as a putative arylsulphatase from *Escherichia coli*. The two structures can be superimposed which an r.m.s.d. on 310 matched C_α atoms of 2.8 Å. The AP superfamily also comprises eukaryotic and prokaryotic sulphatases, as well as phosphodiesterases, mutases and dehydratases, examples of which are all found by SSM in a search of the PDB for structural homologues of LtaS$_{215–649}$.

Table III Crystallographic data collection

Data collection	
Wavelength (Å)	0.9763
Space group	$P\,1\,2_1\,1$
Unit cell parameters	$a = 56.63$ Å, $b = 54.41$ Å, $c = 140.78$ Å, $\beta = 90.97^\circ$
Resolution (Å)	70.36–2.35 (2.48–2.35)
No. of observations	704 196
No. of unique reflections	35 957
Multiplicity	19.6 (7.7)
Anomalous multiplicity	10.1 (3.9)
Completeness (%)	100 (100)
Anomalous completeness	100 (100)
Average *I*/sigma *I*	22.1 (3.8)
R_{sym}	0.124 (0.361)
Refinement	
No. of reflections	34 148
R_{work} (%)	17.1 (21.2)
R_{free} (%)	23.3 (29.9)
No. of atoms	7080
r.m.s.d.	
Bond lengths (Å)	0.012
Bond angles (deg)	1.382
Ramachandran plot	
Favoured (%)	96.1
Allowed (%)	99.9
Mean B-factor	
Wilson B (Å^3)	39.5
Main chain (Å^3)	48.3
Side chain/water (Å^3)	47.3

The overall similarity of LtaS$_{215–649}$ to biochemically characterized enzymes enables the location of the active centre of LtaS to be deduced. First, it was clear immediately on solving the structure that Thr297 is phosphorylated in the crystal (Figure 7; Supplementary Figure 2A). This feature has been refined satisfactorily with unit occupancy and with B-factors similar to nearby, but non-bonded atoms. Second, there is a single metal ion found adjacent to the phosphoryl group that was modelled and refined satisfactorily as magnesium. This metal ion was also present in the crystallization conditions. These electron density features allowed the identification of the active site of LtaS, which resides in the centre of the α/β-domain, with Thr297 situated at the N-terminal end of the central α-helix. The active site is in a cleft on the surface that, in the context of the full-length native protein, would oppose the cell membrane (this is depicted schematically in Figure 7C), the source of phosphatidyl glycerol for LTA synthesis.

To test whether Thr297 was important for LtaS function, we made a mutation that would generate a Thr297Ala substitution. Purification and analysis of the mutant protein showed that phosphorylation was prevented (only one peak at 49.71 kDa, the expected mass for the protein carrying the point mutation). Western blotting of mutant *B. subtilis* cells showed that the protein accumulated to similar levels as the wild-type protein (data not shown). Functionality was assayed by examining the sporulation efficiency when the protein carrying the point mutation was expressed in an otherwise sporulation-deficient *ltaS yqgS* double deletion strain (Table II). The mutant protein was not able to rescue the sporulation-deficient phenotype. We therefore conclude the phosphorylatable Thr297 is essential for LtaS function.

Sequence analysis of the amino acids that are in direct contact with the phosphothreonine at position 297 (His412, Glu253 and Trp350) revealed that they are among the most conserved in LtaS orthologues, suggesting their importance for LTA synthesis. The single magnesium ion in LtaS lies in a distorted octagonal coordination geometry (Figure 7B), coordinated in the equatorial plane by the Nε2 atom of His472, the ether oxygen of phospho-Thr297, and in a bidentate manner by the carboxylate of Glu253, whereas the apical positions are filled by Oδ2 of Asp471 and O1P of phospho-Thr297. A single metal ion is also observed in structures of arylsulphatases (Boltes *et al*, 2001), whereas AP contains three metal ions, only two of which (both zinc) appear to be catalytically active and which straddle the phosphate in a non-covalent enzyme:P_i complexes (reviewed in Galperin and Jedrzejas, 2001). The second of these zinc ions—equivalent in position to the magnesium in LtaS—also coordinates the ether oxygen of the phosphoserine, and is involved in the hydrolysis of the phosphoseryl intermediate (Galperin and Jedrzejas, 2001).

The arylsulphatase group of enzymes are characterized by the unusual requirement for the post-translational formylation of an invariant cysteine, forming Cα-hydroxyformylglycine, to become the active site nucleophile (e.g., Jonas *et al*, 2008). As has been described for alkaline phosphatases, the reaction cycle of the sulphatase subfamily of the AP superfamily also proceeds through a covalent enzyme intermediate—here the nucleophilic Cα-hydroxyformylglycine becomes sulphated (e.g., lysosomal sulphatase; Bond *et al*, 1997). Phospho-Thr297 is spatially equivalent to the

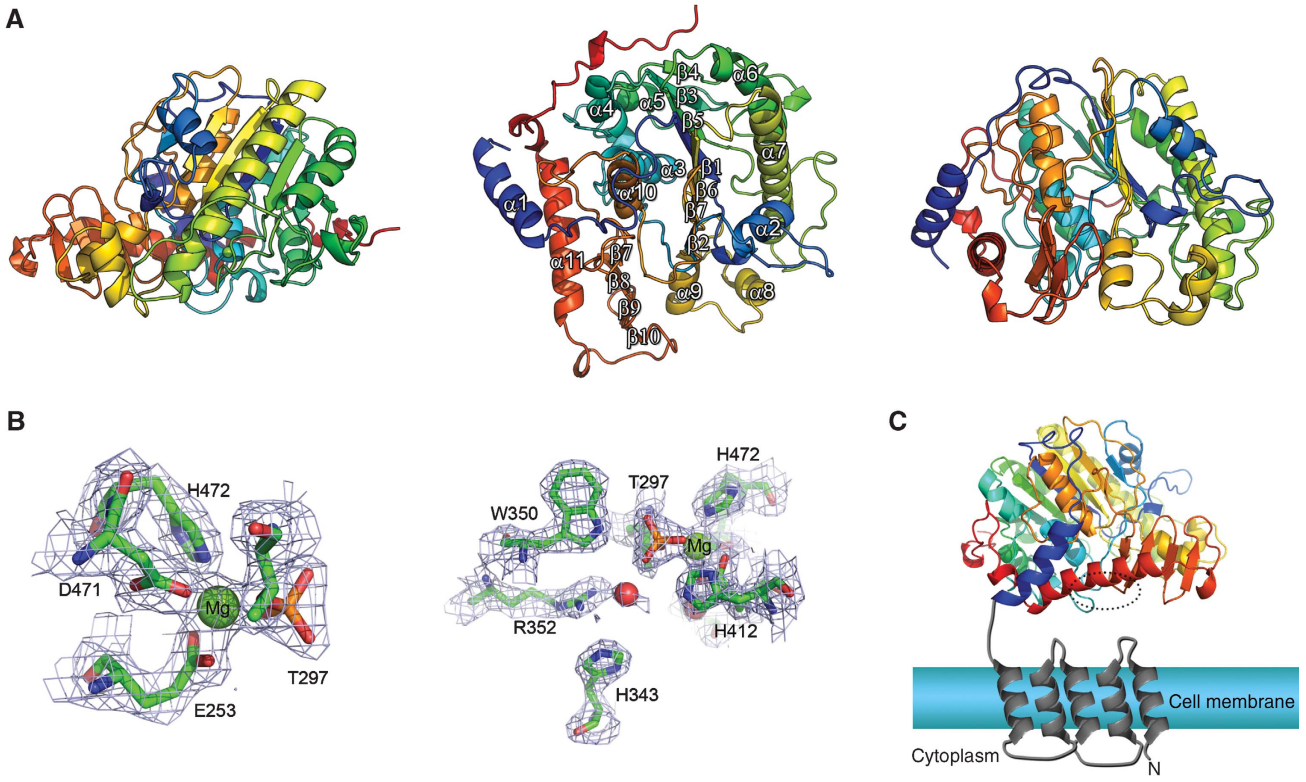

Figure 7 Crystal structure of $LtaS_{215-649}$. (**A**) The protein backbone is rendered as a secondary structure cartoon colour ramped from blue at the N terminus to red at the C terminus. Orthogonal views are shown with the secondary structure elements highlighted in the middle panel. (**B**) The active site of LtaS shown in two views, with residues coordinating the magnesium ion in the active site drawn as sticks with the final REFMAC-weighted $F_{obs}-F_{calc}$ electron density map contoured at 1.5sigma and shown as blue wireframe. (**C**) The domain arrangement of full-length LtaS is illustrated schematically. The N-terminal, trans-membrane spanning helices are modelled, and coloured grey, in the context of a biological membrane. The structure of the C-terminal, catalytic domain of LtaS is drawn as a cartoon, colour-ramped in rainbow manner from N (blue) to C terminus (red). The location of the active site is highlighted by a dotted circle.

Cα-hydroxyformylglycine in sulphatases (Supplementary Figure 1B) and the nucleophilic serine in APs and given that a constellation of Thr297-surrounding amino acids (Glu253, Asp471 and His472) are also conserved in the AP superfamily, we propose that the reaction cycle of LtaS also proceeds through a covalent enzyme intermediate, the adduct of which is likely to be glycerol phosphate. The electron density in the crystallographic maps clearly shows that Thr297 is modified by phosphorylation, not glycerophosphorylation, and MALDI-TOF mass spectroscopy of the protein shows two peaks with a mass difference of 79 Da (peaks at 49 741 and 49 819 kDa, respectively), consistent only with phosphorylation of Thr297. Adjacent to phospho-Thr297 are three water molecules, the positions of two of which may mimic the hydroxyls of a covalently attached glycerol phosphate. One water is in hydrogen bond contact with the side chains of His343, Asn345 and Arg352, the second is in contact with the guanidinium group of Arg352 and the O3P of phospho-Thr297 and the third water contacts the carboxylate of Glu253 and the main chain carbonyl of Thr408. His343, Asn345, Arg352 and Trp350—which sits directly above the phosphoryl group—are highly conserved in LtaS homologues, suggesting that these amino acids have a more important function in catalysis than a simple hydration sphere. Trp350, whose Nε atom contacts two of the phosphoryl oxygens and thus presumably participates in poly(GroP) formation (Figure 7B), is replaced in AP by Arg166, which makes contact with the phosphoryl group during all steps of the reaction cycle (Galperin and Jedrzejas, 2001).

The phosphorylation of Thr297 appears to mimic an intermediate state of the formation of poly(GroP). The source of the phosphorylation, however, is not known. The depth of the pocket in which Thr297 is situated at the base reduces the possibility that LtaS is phosphorylated by a kinase, but instead the source of phosphorylation is likely to be a small molecule phosphodonor, which can phosphorylate two-component response regulators (McCleary *et al*, 1993). The presence of a phosphoryl group on the active centre of the enzyme appears to inhibit LtaS effectively as we could not produce poly(GroP) from glycerol phosphate. LtaS thus seems to have evolved to retain some features of alkaline phosphatase-type enzymes (e.g., covalent phosphoryl enzyme intermediate) and others from the arylsulphatase family (e.g., one-metal hydrolysis, not two or three metal hydrolysis). In fact, the absolute biochemical reaction catalysed by LtaS is not known: most likely the 3′ hydroxyl of an incoming glycerol phosphate moiety attacks the threonyl-glycerophosphate adduct to effect the elimination reaction. Such an in-line attack also invokes a role in catalysis for Lys296, invariant in LtaS homologues, yet its side chain is directed away from the active site ion in our structure. The pocket that is lined by His343, Asn345 and Arg352 is of ideal volume for only a single glycerol (Supplementary Figure 2A, B),

implying that the growing chain of poly(GroP) is the nucleophile in the second stage of the reaction. However, the precise role (indeed, its actual identity) of the bound metal ion in catalysis, how the growing chain is recognized by LtaS and the enzymatic mechanism of poly(GroP) formation and its elimination from LtaS remain unknown and are the subject of further biochemical experimentation.

Conclusions

Despite their importance as almost ubiquitous and abundant components of the walls of Gram-positive bacteria, the functions of TAs have remained the subject of speculation for several decades. Why organisms such as *B. subtilis* produce two distinct forms of TA, linked to the wall and the membrane, has also been unclear. We have now taken several major steps towards answering these questions. First, we have established that although both WTA and LTA are dispensable in *B. subtilis*, jointly, they are essential. This together with recent evidence that LTA is essential in *S. aureus* (which relies largely on the cell division apparatus to enlarge; Pinho and Errington, 2003; Gründling and Schneewind, 2007b) reinforces the notion that TA synthetic enzymes are good potential targets for antibiotics against Gram-positive pathogens. Elucidation of the crystal structure of the catalytic domain of LtaS and identification of its active site residue provide an important framework from which to launch drug discovery programmes. Second, we have shown that the major function of the LTA system lies in divalent cation homoeostasis, in accordance with earlier speculations (Fischer, 1988; Neuhaus and Baddiley, 2003). Third, we have discovered that the WTA and LTA systems have distinct roles in *B. subtilis* cell morphogenesis. It is well known that *B. subtilis* and many other rod-shaped bacteria have distinct morphogenetic systems involved in cell elongation and cell division (e.g., Begg *et al*, 1990; Daniel and Errington, 2003; Claessen *et al*, 2008). Previous work on the WTA system has pointed to a specialized role in elongation, manifested by both a rounded cell phenotype (Wagner and Stewart, 1991; D'Elia *et al*, 2006a) and association of the synthetic enzyme complex with the elongation machinery (Formstone *et al*, 2008). We now show that the *ltaS* mutants are more affected in processes associated with cell division. As WTA and LTA have identical structures in *B. subtilis*, apart from their linkage to PG and membrane, respectively, we assume that it is the spatial distribution of the two polymers that determines their specialized functions. In principle, this means that LTA remains tethered close to the cell membrane surface, whereas the WTA should migrate out through the wall as it matures. As cell division involves ingrowth of the septal membranes, LTA may be especially important in ensuring the availability of Mg^{2+} to synthetic enzymes acting at or near the leading edge of the invaginating septum.

To conclude, this study opens up a number of important new areas of research on the role of LTA and TAs generally, in cell morphogenesis, the cell cycle, sporulation and adaptation to environmental conditions, as well as providing new opportunities for drug discovery.

Materials and methods

For more information on Materials and methods, see Supplementary data. Strains and plasmids are listed in Supplementary Table 1.

Supplementary data

Supplementary data are available at *The EMBO Journal* Online (http://www.embojournal.org).

Acknowledgements

This study was supported by a grant from the UK Biotechnology and Biological Sciences Research Council. We thank the Electron Microscopy Research Services at Newcastle University for their help and Ian Selmes for technical support. We also thank the group members, particularly Ling Juan Wu, Mark Leaver and Jan-Willem Veening for helpful discussions and for a critical reading of the paper. We are grateful for access to the Diamond Light Source and its beamline staff for help during data collection. Coordinates for the crystal structure of LtaS are deposited in the Protein Databank with the accession number 2w8d.

References

Archibald AR, Armstrong JJ, Baddiley J, Hay JB (1961) Teichoic acids and the structure of bacterial walls. *Nature* **191:** 570–572

Arigoni F, Pogliano K, Webb CD, Stragier P, Losick R (1995) Localization of protein implicated in establishment of cell type to sites of asymmetric division. *Science* **270:** 637–640

Barak I, Behari J, Olmedo G, Guzman P, Brown DP, Castro E, Walker D, Westpheling J, Youngman P (1996) Structure and function of the *Bacillus* SpoIIE protein and its localization to sites of sporulation septum assembly. *Mol Microbiol* **19:** 1047–1060

Begg KJ, Takasuga A, Edwards DH, Dewar SJ, Spratt BG, Adachi H, Ohta T, Matsuzawa H, Donachie WD (1990) The balance between different peptidoglycan precursors determines whether *Escherichia coli* cells will elongate or divide. *J Bacteriol* **172:** 6697–6703

Bhavsar AP, Brown ED (2006) Cell wall assembly in *Bacillus subtilis*: how spirals and spaces challenge paradigms. *Mol Microbiol* **60:** 1077–1090

Bhavsar AP, Erdman LK, Schertzer JW, Brown ED (2004) Teichoic acid is an essential polymer in *Bacillus subtilis* that is functionally distinct from teichuronic acid. *J Bacteriol* **186:** 7865–7873

Blackman SA, Smith TJ, Foster SJ (1998) The role of autolysins during vegetative growth of *Bacillus subtilis* 168. *Microbiology* **144:** 73–82

Boltes I, Czapinska H, Kahnert A, von Bülow R, Dierks T, Schmidt B, von Figura K, Kertesz MA, Usón I (2001) 1.3 Å structure of arylsulfatase from *Pseudomonas aeruginosa* establishes the catalytic mechanism of sulfate ester cleavage in the sulfatase family. *Structure* **9:** 483–491

Bond CS, Clements PR, Ashby SJ, Collyer CA, Harrop SJ, Hopwood JJ, Guss MJ (1997) Structure of a human lysosomal sulphatase. *Structure* **5:** 227–289

Carballido-López R (2006) The bacterial actin-like cytoskeleton. *Microbiol Mol Biol Rev* **70:** 888–909

Carballido-López R, Formstone A, Li Y, Ehrlich SD, Noirot P, Errington J (2006) Actin homolog MreBH governs cell morphogenesis by localization of the cell wall hydrolase LytE. *Dev Cell* **11:** 399–409

Carniol K, Ben-Yehuda S, King N, Losick R (2005) Genetic dissection of the sporulation protein SpoIIE and its role in asymmetric division in *Bacillus subtilis*. *J Bacteriol* **187:** 3511–3520

Cheung HY, Freese E (1985) Monovalent cations enable cell wall turnover of the turnover-deficient *lyt*-15 mutant of *Bacillus subtilis*. *J Bacteriol* **161:** 1222–1225

Claessen D, Emmins R, Hamoen LW, Daniel RA, Errington J, Edwards DH (2008) Control of the cell elongation–division cycle by shuttling of PBP1 protein in *Bacillus subtilis*. *Mol Microbiol* **68:** 1029–1046

Cowan JA (1995) *Biological Chemistry of Magnesium*. New York: Wiley-VCH

D'Elia MA, Millar KE, Beveridge TJ, Brown ED (2006a) Wall teichoic acid polymers are dispensable for cell viability in *Bacillus subtilis*. *J Bacteriol* **188:** 8313–8316

D'Elia MA, Pereira MP, Chung YS, Zhao W, Chau A, Kenney TJ, Sulavik MC, Black TA, Brown ED (2006b) Lesions in teichoic acid biosynthesis in *Staphylococcus aureus* lead to a lethal gain of function in the otherwise dispensable pathway. *J Bacteriol* **188:** 4183–4189

Dajkovic A, Lutkenhaus J (2006) Z ring as executor of bacterial cell division. *J Mol Microbiol Biotechnol* **11:** 140–151

Daniel RA, Errington J (2003) Control of cell morphogenesis in bacteria: two distinct ways to make a rod-shaped cell. *Cell* **113:** 767–776

Den Blaauwen T, de Pedro MA, Nguyen-Disteche M, Ayala JA (2008) Morphogenesis of rod-shaped sacculi. *FEMS Microbiol Rev* **32:** 321–344

Dziarski R (2003) Recognition of bacterial peptidoglycan by the innate immune system. *Cell Mol Life Sci* **60:** 1793–1804

Errington J (1993) *Bacillus subtilis* sporulation: regulation of gene expression and control of morphogenesis. *Microbiol Mol Biol Rev* **57:** 1–33

Errington J (2003) Regulation of endospore formation in *Bacillus subtilis*. *Nat Rev Microbiol* **1:** 117–126

Fedtke I, Götz F, Peschel A (2004) Bacterial evasion of innate host defenses—the *Staphylococcus aureus* lesson. *Int J Med Microbiol* **294:** 189–194

Fischer W (1988) Physiology of lipoteichoic acids in bacteria. *Adv Microb Physiol* **29:** 233–302

Fittipaldi N, Sekizaki T, Takamatsu D, Harel J, Domínguez-Punaro Mde L, Von Aulock S, Draing C, Marois C, Kobisch M, Gottschalk M (2008) D-alanylation of lipoteichoic acid contributes to the virulence of *Streptococcus suis*. *Infect Immun* **76:** 3587–3594

Formstone A, Carballido-Lopez R, Noirot P, Errington J, Scheffers D-J (2008) Localization and interactions of teichoic acid synthetic enzymes in *Bacillus subtilis*. *J Bacteriol* **190:** 1812–1821

Formstone A, Errington J (2005) A magnesium-dependent *mreB* null mutant: implications for the role of *mreB* in *Bacillus subtilis*. *Mol Microbiol* **55:** 1646–1657

Galperin MY, Jedrzejas MJ (2001) Conserved core structure and active site residues in alkaline phosphatase superfamily enzymes. *Proteins* **45:** 318–324

Glenn AR, Mandelstam J (1971) Sporulation in *Bacillus subtilis* 168. Comparison of alkaline phosphatase from sporulating and vegetative cells. *Biochem J* **123:** 129–138

Gross M, Cramton SE, Götz F, Peschel A (2001) Key role of teichoic acid net charge in *Staphylococcus aureus* colonization of artificial surfaces. *Infect Immun* **69:** 3423–3426

Gründling A, Schneewind O (2007a) Genes required for glycolipid synthesis and lipoteichoic acid anchoring in *Staphylococcus aureus*. *J Bacteriol* **189:** 2521–2530

Gründling A, Schneewind O (2007b) Synthesis of glycerol phosphate lipoteichoic acid in *Staphylococcus aureus*. *Proc Natl Acad Sci USA* **104:** 8478–8483

Henriques AO, Glaser P, Piggot PJ, Moran Jr CP (1998) Control of cell shape and elongation by the *rodA* gene in *Bacillus subtilis*. *Mol Microbiol* **28:** 235–247

Heptinstall S, Archibald AR, Baddiley J (1970) Teichoic acids and membrane function in bacteria. *Nature* **225:** 519–521

Hilbert DW, Piggot PJ (2004) Compartmentalization of gene expression during *Bacillus subtilis* spore formation. *Microbiol Mol Biol Rev* **68:** 234–262

Hirose I, Sano K, Shioda I, Kumano M, Nakamura K, Yamane K (2000) Proteome analysis of *Bacillus subtilis* extracellular proteins: a two-dimensional protein electrophoretic study. *Microbiology* **146:** 65–75

Hofmann K, Stoffel W (1993) Tmbase—a database of membrane spanning proteins segments. *Biol Chem Hoppe-Seyler* **374:** 166

Höltje JV (1998) Growth of the stress-bearing and shape-maintaining murein sacculus of *Escherichia coli*. *Microbiol Mol Biol Rev* **62:** 181–203

Illing N, Errington J (1991) Genetic regulation of morphogenesis in *Bacillus subtilis*: roles of σ^E and σ^F in prespore engulfment. *J Bacteriol* **173:** 3159–3169

Jervis AJ, Thackray PD, Houston CW, Horsburgh MJ, Moir A (2007) SigM-responsive genes of *Bacillus subtilis* and their promoters. *J Bacteriol* **189:** 4534–4538

Jonas S, van Loo B, Hyvönen M, Hollfelder F (2008) A new member of the alkaline phosphatase superfamily with a formylglycine nucleophile: structural and kinetic characterisation of a phosphonate monoester hydrolase/phosphodiesterase from *Rhizobium leguminosarum*. *J Mol Biol* **384:** 120–136

Jones LJ, Carballido-López R, Errington J (2001) Control of cell shape in bacteria: helical, actin-like filaments in *Bacillus subtilis*. *Cell* **104:** 913–922

Khvorova A, Zhang L, Higgins ML, Piggot PJ (1998) The *spoIIE* locus is involved in the Spo0A-dependent switch in the location of FtsZ rings in *Bacillus subtilis*. *J Bacteriol* **180:** 1256–1260

Koch AL (1985) How bacteria grow and divide in spite of internal hydrostatic pressure. *Can J Microbiol* **31:** 1071–1084

Koch AL (2003) Bacterial wall as target for attack: past, present, and future research. *Clin Microbiol Rev* **16:** 673–687

Koch AL (2006) The exocytoskeleton. *J Mol Microbiol Biotechnol* **11:** 115–125

Kovacs M, Halfmann A, Fedtke I, Heintz M, Peschel A, Vollmer W, Hakenbeck R, Bruckner R (2006) A functional *dlt* operon, encoding proteins required for incorporation of D-alanine in teichoic acids in Gram-positive bacteria, confers resistance to cationic antimicrobial peptides in *Streptococcus pneumoniae*. *J Bacteriol* **188:** 5797–5805

Kristian SA, Lauth X, Nizet V, Götz F, Neumeister B, Peschel A, Landmann R (2003) Alanylation of teichoic acids protects *Staphylococcus aureus* against Toll-like receptor 2-dependent host defense in a mouse tissue cage infection model. *J Infect Dis* **188:** 414–423

Lazarevic V, Karamata D (1995) The *tagGH* operon of *Bacillus subtilis* 168 encodes a two-component ABC transporter involved in the metabolism of two wall teichoic acids. *Mol Microbiol* **16:** 345–355

Leaver M, Errington J (2005) Roles for MreC and MreD proteins in helical growth of the cylindrical cell wall in *Bacillus subtilis*. *Mol Microbiol* **57:** 1196–1209

Mauël C, Young M, Karamata D (1991) Genes concerned with synthesis of poly(glycerol phosphate), the essential teichoic acid in *Bacillus subtilis* strain 168, are organized in two divergent transcription units. *J Gen Microbiol* **137:** 929–941

McCleary WR, Stock JB, Ninfa AJ (1993) Is acetyl phosphate a global signal in *Escherichia coli*. *J Bacteriol* **175:** 2783–2798

Mendelson NH, Thwaites JJ, Favre D, Surana U, Briehl MM, Wolfe A (1985) Factors contributing to helical shape determination and maintenance in *Bacillus subtilis* macrofibres. *Ann Inst Pasteur Microbiol* **136A:** 99–103

Millán JL (2006) Alkaline phosphatases: structure, substrate specificity and functional relatedness to other members of a large superfamily of enzymes. *Purinergic Signal* **2:** 335–341

Morath S, Geyer A, Hartung T (2001) Structure–function relationship of cytokine induction by lipoteichoic acid from *Staphylococcus aureus*. *J Exp Med* **193:** 393–397

Moszer I, Jones LM, Moreira S, Fabry C, Danchin A (2002) SubtiList: the reference database for the *Bacillus subtilis* genome. *Nucleic Acids Res* **30:** 62–65

Neuhaus FC, Baddiley J (2003) A continuum of anionic charge: structures and functions of D-alanyl teichoic acids in Gram-positive bacteria. *Microbiol Mol Biol Rev* **67:** 686–723

Nouaille S, Commissaire J, Gratadoux JJ, Ravn P, Bolotin A, Gruss A, Le Loir Y, Langella P (2004) Influence of lipoteichoic acid D-alanylation on protein secretion in *Lactococcus lactis* as revealed by random mutagenesis. *Appl Environ Microbiol* **70:** 1600–1607

Oku Y, Kurokawa K, Matsuo M, Yamada S, Lee BL, Sekimizu K (2009) Pleiotropic roles of polyglycerolphosphate synthase of lipoteichoic acid in growth of *Staphylococcus aureus* cells. *J Bacteriol* **191:** 141–151

Paulton RJ (1971) Nuclear and cell division in filamentous bacteria. *Nat New Biol* **231:** 271–274

Perego M, Glaser P, Minutello A, Strauch MA, Leopold K, Fischer W (1995) Incorporation of D-alanine into lipoteichoic acid and wall teichoic acid in *Bacillus subtilis*. Identification of genes and regulation. *J Biol Chem* **270:** 15598–15606

Piggot PJ, Coote JG (1976) Genetic aspects of bacterial endospore formation. *Microbiol Mol Biol Rev* **40:** 908–962

Pinho MG, Errington J (2003) Dispersed mode of *Staphylococcus aureus* cell wall synthesis in the absence of the division machinery. *Mol Microbiol* **50:** 871–881

Schaffer C, Messner P (2005) The structure of secondary cell wall polymers: how Gram-positive bacteria stick their cell walls together. *Microbiology* **151:** 643–651

Schertzer JW, Brown ED (2003) Purified, recombinant TagF protein from *Bacillus subtilis* 168 catalyzes the polymerization of glycerol phosphate onto a membrane acceptor *in vitro*. *J Biol Chem* **278:** 18002–18007

Schirner K, Errington J (2009) The cell wall regulator sI specifically suppresses the lethal phenotype of mbl mutants in Bacillus subtilis. *J Bacteriol* **191** (in press; doi:10.1128/JB.01497-08)

Seo HS, Michalek SM, Nahm MH (2008) Lipoteichoic acid is important in innate immune responses to Gram-positive bacteria. *Infect Immun* **76:** 206–213

Smith TJ, Blackman SA, Foster SJ (2000) Autolysins of *Bacillus subtilis*: multiple enzymes with multiple functions. *Microbiology* **146:** 249–262

Stewart GC (2005) Taking shape: control of bacterial cell wall biosynthesis. *Mol Microbiol* **57:** 1177–1181

Stragier P, Bouvier J, Bonamy C, Szulmajster J (1984) A developmental gene product of *Bacillus subtilis* homologous to the sigma factor of *Escherichia coli*. *Nature* **312:** 376–378

Thompson LS, Beech PL, Real G, Henriques AO, Harry EJ (2006) Requirement for the cell division protein DivIB in polar cell division and engulfment during sporulation in *Bacillus subtilis*. *J Bacteriol* **188:** 7677–7685

Vollmer W, Blanot D, de Pedro MA (2008) Peptidoglycan structure and architecture. *FEMS Microbiol Rev* **32:** 149–167

Wagner PM, Stewart GC (1991) Role and expression of the *Bacillus subtilis rodC* operon. *J Bacteriol* **173:** 4341–4346

Wecke J, Madela K, Fischer W (1997) The absence of D-alanine from lipoteichoic acid and wall teichoic acid alters surface charge, enhances autolysis and increases susceptibility to methicillin in *Bacillus subtilis*. *Microbiology* **143:** 2953–2960

Wei Y, Havasy T, McPherson DC, Popham DL (2003) Rod shape determination by the *Bacillus subtilis* class B penicillin-binding proteins encoded by *pbpA* and *pbpH*. *J Bacteriol* **185:** 4717–4726

Weidenmaier C, Kokai-Kun JF, Kristian SA, Chanturiya T, Kalbacher H, Gross M, Nicholson G, Neumeister B, Mond JJ, Peschel A (2004) Role of teichoic acids in *Staphylococcus aureus* nasal colonization, a major risk factor in nosocomial infections. *Nat Med* **10:** 243–245

Wu LJ, Errington J (1994) *Bacillus subtilis* SpoIIIE protein required for DNA segregation during asymmetric cell division. *Science* **264:** 572–575

Wu LJ, Errington J (1998) Use of asymmetric cell division and *spoIIIE* mutants to probe chromosome orientation and organization in *Bacillus subtilis*. *Mol Microbiol* **27:** 777–786

